

Fig 6

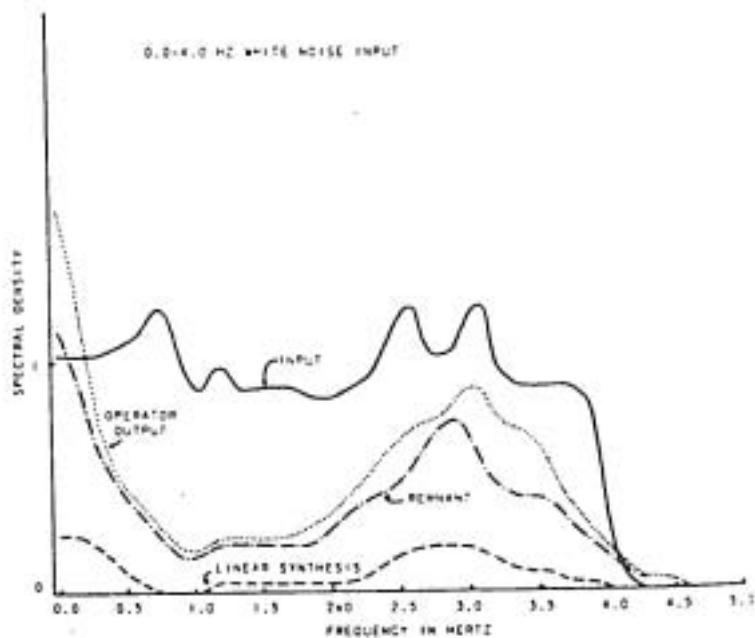


Fig 7

## A REVISED CONCEPTION OF VISUAL RECEPTIVE FIELDS

## BASED ON PSEUDORANDOM SPATIO-TEMPORAL PATTERN STIMULI

Erich Sutter

## 1. Introduction

The concept of the receptive field originated in somesthesia. There the receptive field of a neuron was defined as the skin area from which a tactile stimulus would influence the firing pattern of a neuron. Researchers in vision took over the concept to denote those areas of the retina from which a cell receives its excitatory or inhibitory input.

Most of the research in the mammalian visual system concerns itself with receptive fields in one way or another. In the more conventional experiments stimuli are projected onto a screen in front of the immobilized eyes of the animal preparation, while a single neuron in the visual system is monitored. Some researchers (7, 8) probe the visual field of the animal with a hand projector to find out the approximate size of the excitatory and inhibitory areas. Other investigators (3, 4, 10, 11, 12) arrived at a more quantitative method by recording the responses to a certain basic set of stimuli. A good example is Spinelli's technique from our laboratory. Here the responses to a small light or dark spot stimulus are recorded in 2,500 evenly distributed, sequential spot positions. In a computer generated display those positions in the visual field for which the response exceeds a certain threshold are marked with light spots (Fig. 1).

Generally a moving or flashing stimulus is used, since most cells seem to respond to changes in the physical stimulus rather than to the geometry of the stimulus itself. Except for this point the time dimension has not entered into these receptive field studies. In other experiments, however, the average delay time between stimulus and response has been measured (2, 5, 6, 13). Although a large amount of valuable information has been gathered with these methods, it seems unlikely that they will be powerful enough to convey an adequate understanding of the system at hand. This may be the time to go beyond the all too restrictive concepts of receptive field and time delay and face the general problem of determining the transfer characteristics of the visual system as defined by visual input and single unit response. Since such systems have a certain amount of "memory" and may be nonlinear, the use of the Wiener method for nonlinear systems and identification (1, 14) seems indicated.

## 2. Input

Color stimuli will not be discussed here since the cat, on which the experiments were performed, rarely shows color vision when tested behaviorally. Everything said here can, at a later time, be generalized for the investigation of color vision in primates. Thus the input to the system is given by a simple light intensity function  $I(x, y, t)$  where  $x$  and  $y$  are the two dimensions of the visual field. The light intensity is a positive definite function. However, the response does not seem to depend on the average light intensity, at least as long as the stimulus remains within either the photopic or the scotopic

range. The zero level of the light intensity can thus be redefined at the level of the average light intensity. The set of functions  $I(x, y, t)$  can then be chosen as the  $L^2$  space of square integrable intensities. The scalar product

$$(I_1, I_2)_t = \iint dx dy I_1(x, y, t) I_2(x, y, t) \quad (3)$$

then allows the choice of orthonormal bases.

Let us assume temporarily that the system we are dealing with has negligible memory. In this case the response at time  $t$  ( $R(t)$ ) depends only on the intensity pattern  $I(x, y, t - \tau)$ , where  $\tau$  is the time delay. The only relevant temporal information concerning the system is thus the delay time  $\tau$ . All other information is purely spatial and consists in the specification of the strength and sign (inhibitory or excitatory) of the inputs from different retinal points. It is described by the functional

$$R = F \{ I(x, y) \} \quad (4)$$

If, furthermore, the transfer characteristics are linear, this can be represented by the integral

$$R = \iint dx dy r(x, y) I(x, y) \quad (5)$$

For the determination of  $r(x, y)$  it is sufficient to test the system with a complete orthonormal set of intensity functions  $\{i_k(x, y) | k = 1, \dots, n\}$ , as given, e.g. by a series of sine wave gratings in the  $x$  and  $y$  direction up to the cutoff frequency of the system, or by a small spot in a large number of evenly spaced positions as used in the Spinelli technique mentioned earlier.

Unfortunately neither linearity nor zero memory can be assumed for the description of the single unit response to visual stimuli. A complete orthonormal set is therefore by no means adequate for the investigation of the transfer characteristics

$$R(\tau) = F \{ I(x, y, t); \tau \} \quad (6)$$

We have to reach for a much larger stimulus arsenal, namely an ergodic stimulus as given by spatio-temporal Gaussian white noise. Such a stimulus approximates all possible spatio-temporal configurations within the relevant dynamic range to a sufficient degree of accuracy with a time interval of order length.

### 3. Output

The response of the system consists of a temporal pattern of action potentials which often occur in bursts. The same pattern can generally be reproduced by repetition of the same visual stimulus sequence. Behind this fact may lie one or several of the following reasons; first, other uncontrolled inputs to the system; second, spontaneous activity of the system itself; and third, the probabilistic nature of the functional properties of its components. It seems therefore necessary to obtain the probability density for action potentials by repeated playing of the same noise stimulus. Once an adequate approximation to the density is obtained it can be treated just like a continuous response.

#### 4. Wiener kernels

Under the assumption of translational invariance in time, the functional power series expansion of  $R(I)$  results in the Volterra series:

$$R(t) = h_0 + \int dx dy d\tau h_1(x, y, t-\tau) I(x, y, \tau) \quad (5)$$

$$+ \int dx dy d\tau \int dx' dy' d\tau' h_2(x, y, t-\tau; x', y', t-\tau') I(x, y, \tau) I(x', y', \tau')$$

$$+ \dots$$

Causality demands that  $h_i = 0$  for  $t < t^i$ .

The kernels  $h_i$  can be determined by cross correlation (9):

$$h_0 = E[R(t)] \quad \text{average firing rate}$$

$$h_1(x, y, \tau) = \frac{1}{p} E[R(t) I(x, y, t-\tau)] \quad (6)$$

$$h_2(x, y, \tau; x', y', \tau') = \frac{1}{p^2} E[R(t) I(x, y, t-\tau) I(x', y', t-\tau')]$$

$$h_3, \dots \quad \text{where } p \text{ is the power level of the white noise input}$$

The enormously high dimensionality of the higher order kernels makes complete calculation of kernels of higher than first or second order virtually impossible. However, certain matrix elements which may be of particular interest could be individually calculated.

If the probability density of spike responses is not accessible, single bursts (or spikes) can be interpreted as discrete responses. The response onset can be accurately defined by the first spike in the burst while the strength of the response is given by the number of spikes in the burst. The resulting response function is given by

$$R(t) = \sum_i a_i \delta(t-t_i) \quad (7)$$

$a_i$  = strength of the  $i^{\text{th}}$  response  
 $t_i$  = time of the  $i^{\text{th}}$  response

The expressions for the first three Wiener kernels then become:

$$h_0 = \frac{1}{n} \sum_{i=1}^n a_i \quad \text{average response strength} \quad (8)$$

$$h_1(x, y, \tau) = \frac{1}{n} \sum_{i=1}^n a_i I(x, y, t_i - \tau) \quad \text{response related weighted average of stimulus epochs}$$

$$h_2(x, y, \tau; x', y', \tau') = \frac{1}{n} \sum_{i=1}^n a_i^2 I(x, y, t_i - \tau) I(x', y', t_i - \tau')$$

spatio-temporal covariance matrix

Dealing with this type of discrete response rather than with spike probability densities definitely has its drawbacks. It is not likely that good results will be produced when the firing rate of the cell is primarily inhibited by the stimulus. In such instances the absence of spikes has to be interpreted as a response. Absences, however, are impossible to define if the average firing rate is already low, as in the case of many cortical cells.

### 5. Pilot Study

In the preliminary study certain simplifying assumptions were made mainly in order to meet the limitations of the available equipment. First, producing a continuous spatio-temporal white noise stimulus is no trivial matter. One obstacle is the flicker produced by ordinary TV scan and motion picture film. A simple way to produce a continuous noise stimulus consists in adding white noise to the x, y and intensity inputs of the display scope. Although a stimulus does not meet the spectral requirements of Gaussian white noise, it proved adequate for obtaining a rough estimate of  $h_1$ .

In this experiment the responses were considered discrete. A pulse analyzer was designed to select bursts and measure their strength by counting the number of spikes. The functioning of the analyzer is explained in Fig. 2.

Fig. 3 shows the general arrangement used for the recording session. A single tape is run through two adjacent tape recorders. The one on the right reproduces the stimulus while the one on the left records the single unit response on a different track of the same tape. Note that the temporal relationship between stimulus and response is preserved.

In the subsequent data processing the arrangement shown in Fig. 4 is used.

The stimulus is played back just as in recording session except for the fact that the brightness input  $z$  is only triggered for a 3 ms interval whenever the pulse analyzer detects a response in the recorded firing pattern of the cell. The brightness pulse is proportional to the number of spikes in the response such that the brightness of the display is weighted according to the strength of response to which it is related. By adjusting the distance between the two tape recorders with the help of the microdrive, the 3 ms interval of display can be chosen to precede the response by a given time  $T$ . It can thus be made to occur anywhere within the stimulus epoch relevant to the response (Fig. 5).

A camera with an open shutter located in front of the scope screen records the averaging by summing up all the 3 ms flashes displayed.

For every setting of the advance time  $T$  an average picture is obtained. By varying  $T$  in small steps, the whole relevant stimulus epoch can be scanned. Thus a sequence of photographs is obtained which illustrates the spatio-temporal structure of the average response related stimulus epoch.

The question arises as to how long a recording session has to be continued to produce adequate results. In the case of a finite sample, the estimate  $M_n$  of the first Wiener kernel  $h_1$  is equal to the sample mean

$$M_n = \frac{1}{n} \sum_{i=1}^n \frac{1}{p} a_i f(x, y, t_i - \tau) \quad (4)$$

the random variable

$$X = \frac{1}{p} a_i I(x, y, t_i - \tau) \quad (10)$$

ance

$$\text{Var } M_n = \frac{1}{n} \text{Var } X \quad (11)$$

we have

$$\text{Var } \hat{h}_1(\tau) = \frac{1}{n} \text{Var} \left[ \frac{1}{p} a_i I(x, y, t_i - \tau) \right] \quad (12)$$

The variance of the stimulus input itself can be taken as an upper bound for the variance  $I(x, y, t_i - T)$  at the fix point  $(x, y)$ . If 2,500 equally spaced points are to be resolved on the display screen, it can be assumed that perhaps a thousand of these are the origin of an appreciable input to the cell. On the average, each input thus contributes one-thousandth of the total response. If three intensity levels are to be resolved, the number  $n$  of samples in formula (12) above for the variance of the estimate has to be chosen larger than 3,000. The average response rate is of the order of one per second such that the time required for the collection of 3,000 samples amounts to about 50 minutes.

This is a very rough estimate. The fact that the thousand inputs do not contribute equally reduces the required time. On the other hand, not all responses are stimulus related, since the input-output relationship is contaminated with other, unknown inputs as well as spontaneous activity. This contamination, of course, requires a lengthening of the recording time.

The results shown in Fig. 6 were obtained from a half-hour record of a simple cell from the primary visual cortex of the cat. The pictures represent a computer processed version of the photographs and distinguish 2,500 points, each with three discrete intensity levels. The poor spatial resolution is partly due to inaccurate reproduction of the stimulus in different replays. The variance in the position of the scope trace amounted to more than 10 percent of the horizontal dimension. With better equipment and the real spatio-temporal Gaussian white noise stimulus, a much higher resolution could be expected from a record of the same length.

It seemed necessary to devise an experimental test for the spatial and temporal resolution of which the experimental set-up is capable. For this purpose a simulator with very well defined transfer characteristics was designed. Its function is illustrated in Fig. 7.

Two photo diodes monitor the average light intensity of two parallel bars in the visual field. If the light intensities reach their respective threshold two "neurons" A and B fire with a time delay  $T$ . A connection from B to A inhibits A whenever B fires. This inhibition arrives at A with a delay of 10 ms and lasts for a period of 12 ms. A, which is being monitored, will therefore fire at some arbitrary time  $t$  if and only if the light intensity on bar I exceeds threshold at time  $t-T$  and the light intensity on bar II was below threshold from time  $t-T-10\text{ms}$  to  $t-T-22\text{ms}$ . The estimate for  $h_1$  obtained from a 10-minute record shows that the average stimulus epoch in the experiment approximates the predicted spatio-temporal structure quite well (Fig. 8).

## 6. Conclusion

The pilot study showed that, in spite of the large number of inputs

which have to be resolved for adequate spatial resolution, a Wiener-type analysis can be expected to produce results from recording sessions lasting one or two hours. In order to make the investigation more quantitative and to extend it to the second order Wiener kernel, it will be necessary to develop a highly reproducible and well defined spatio-temporal Gaussian white noise stimulus. The same stimulus should be presented several times in order to obtain a continuous spike density function for processing. If the individual response records are stored separately, the Wiener method could even be refined for a more detailed investigation of the response structure. With colored noise and an adequate increase in record length, the technique is readily adapted to the investigation of color vision in primates.

#### References

1. Barrett, J. F. The use of functional in the analysis of nonlinear physical systems. J. Electron. Control, 15: 567-615, 1963.
2. Cleland, B. G., Dubin, M. W. and Levick, W. R. Sustained and transient neurons in the cat's retina and lateral geniculate nucleus. J. Physiol., 217, 1970.
3. Creutzfeldt, O. and Ito, M. Functional synaptic organization of primary visual cortex neurones in the cat. Exp. Brain Res., 6, 1968.
4. Enroth-Cugell, C. and Robson, J. G. The contrast sensitivity of retinal ganglion cells in the cat. J. Physiol., 187, 1966.
5. Hisako, K. and Wright, M. Y. Receptive field organization of "sustained" and "transient" retinal ganglion cells which subserve different functional roles. J. Physiol., 227: 769-800, 1972.
6. Hoffmann, K. Conduction velocity in pathways from retina to superior colliculus in the cat: a correlation with receptive-field properties. J. Neurophysiol., 36(3): 1973.
7. Hubel, D. H. and Wiesel, R. N. Receptive fields and functional architecture of monkey striate cortex. J. Physiol., 195, 1968.
8. Kuffler, S. W. Discharge patterns and functional organization of mammalian retina. J. Neurophysiol., 16, 1953.
9. Lee, Y. W. and Schetzen, M. Measurement of the kernels of a non-linear system by crosscorrelation. Quart. Progr. Rept. Res. Lab. Electron. 1961.
10. Pettigrew, J. D., Nikara, T. and Bishop, R. O. Responses to moving slits by single units in cat striate cortex. Exp. Brain Res., 6, 1966.
11. Phelps, R. W. The effect of spatial and temporal interactions on the response of single units in the cat's visual cortex. Intern. J. Neurophysiol. press.
12. Spinelli, D. N. Receptive field organization of ganglion cells in the cat's retina. Exp. Neurology, 19(3), 1967.

3. Stone, J. and Dreher, B. Projection of X- and Y-cells of the cat's lateral geniculate nucleus to areas 17 and 18 of visual cortex. J. Neurophysiol., 36(3), 1973.

4. Wiener, N. Nonlinear Problems in Random Theory. New York: Wiley and Sons, 1958.



### FIGURE LEGENDS

1. Example of a plot obtained with the Spinelli technique.
2. Actual scope traces illustrating the function of the pulse analyzer. If two subsequent spikes do not fall within a given time interval  $T_1$  the criterion for the onset of a response is not met. No output is generated (top frame). If the criterion is met (bottom frame), an integrator steps up the voltage with every spike. At time interval  $T_2$ , after the first spike, a 3 ms pulse proportional to the resulting level is generated at the output.
3. The recording arrangement.
4. The processing arrangement.
5. The top line symbolizes the stimulus, the bottom line the corresponding discrete responses. The stimulus epoch which is related to the response is filled in black. A 3 ms section (initiated by hatching) is flashed onto the display screen with an intensity proportional to the strength of the corresponding response. Photographic summation of all the flashes results in a single frame out of the average stimulus epoch.
6. Average stimulus epoch of a simple cell in the primary visual cortex of the cat. The zero point for the time indicated in milliseconds below each frame is the first spike of the response burst.
7. The function of the test simulator (See text).
8. Average stimulus epoch obtained with the test simulator. The common time delay (See Figure 7) which only produces an overall shift in time has been chosen to be zero. The first frame indicates the actual outlines of the two bars.

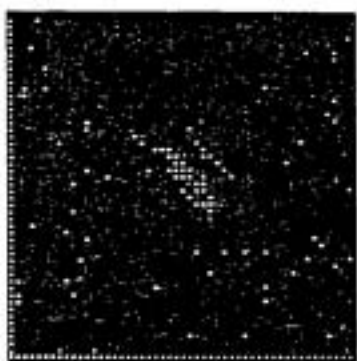


Fig. 1

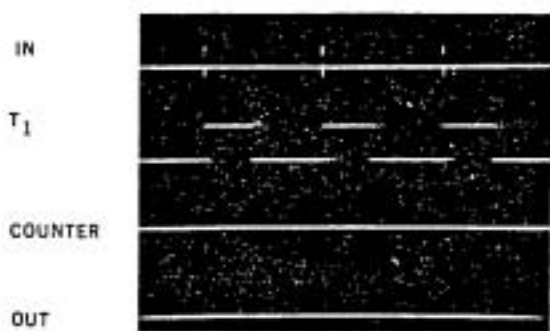


Fig. 2

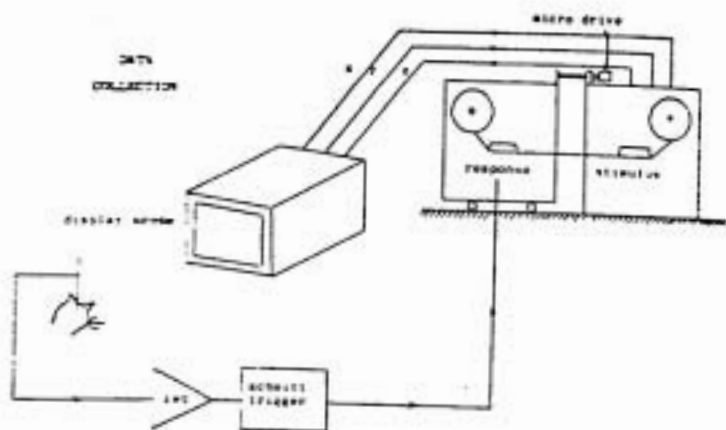


Fig. 3

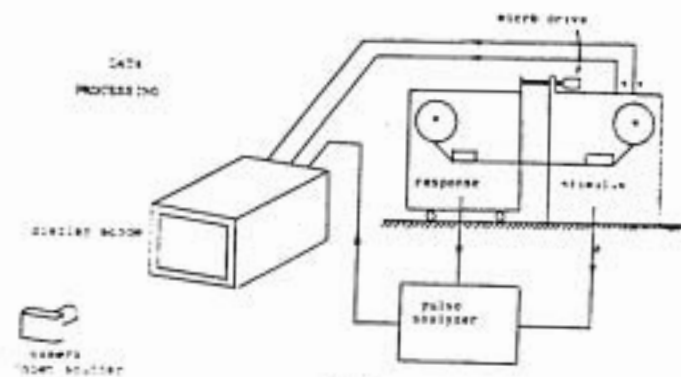


Fig. 4

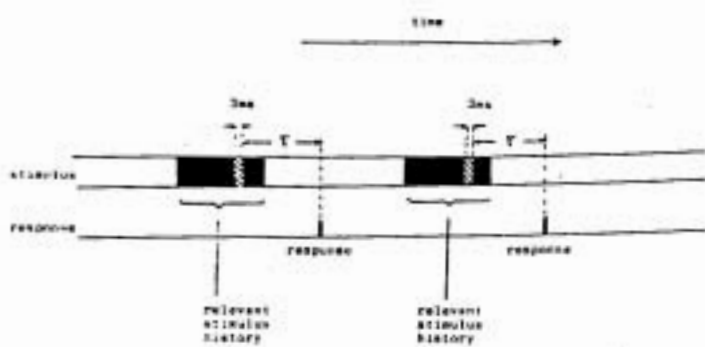


Fig. 5

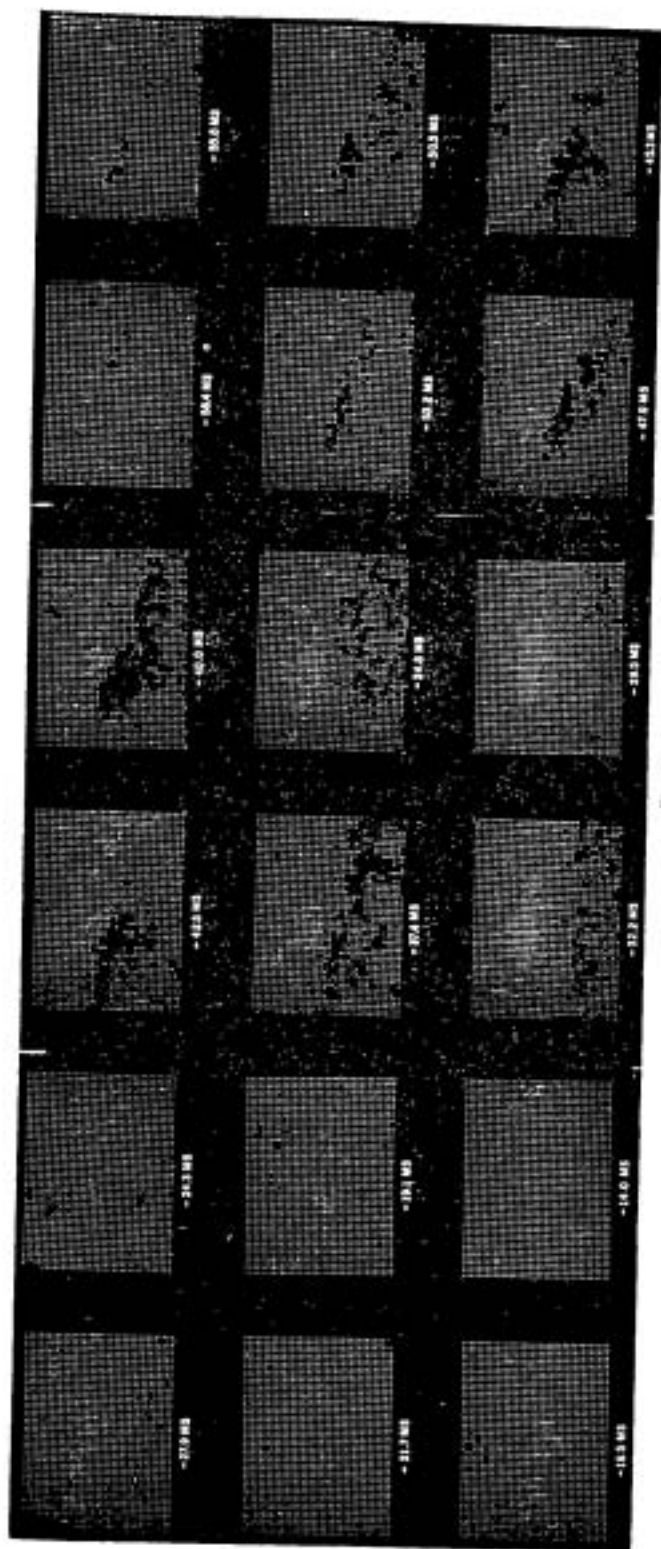


Fig. 6

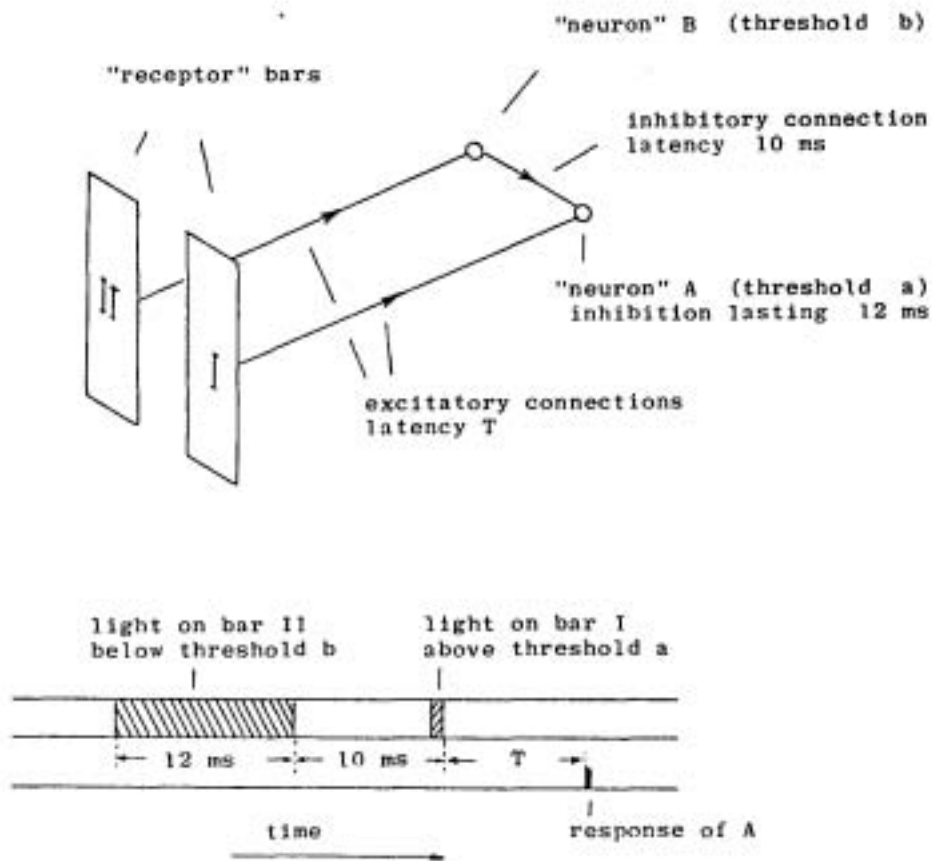
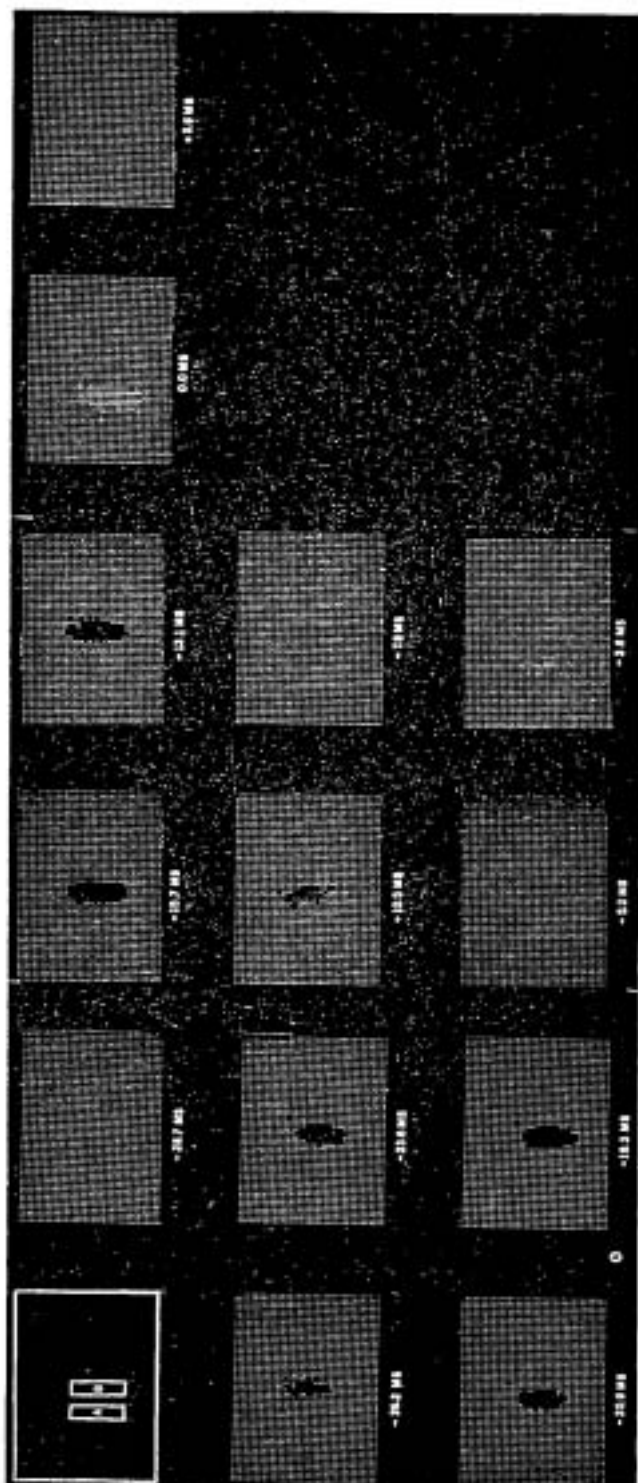
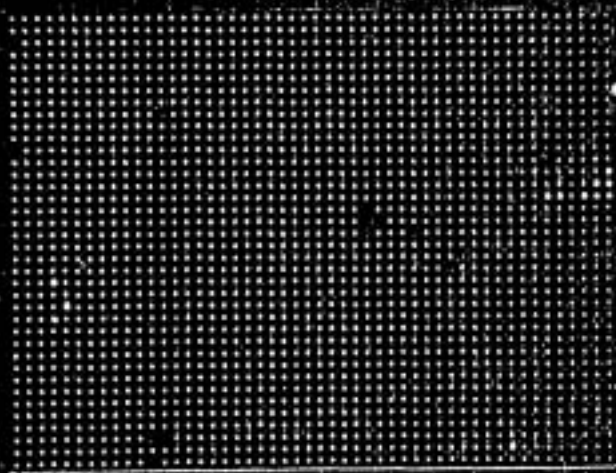
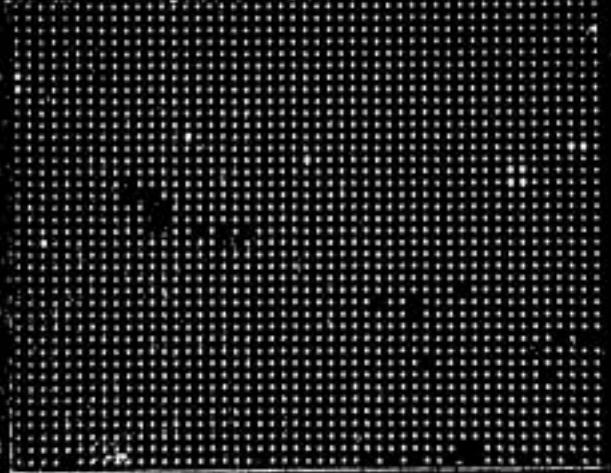
SIMULATION

Fig. 7





- 58.4 MS



- 55.8 MS



- 53.2 MS



- 50.5 MS



- 47.9 MS



- 45.3 MS



- 42.6 MS



- 40.0 MS



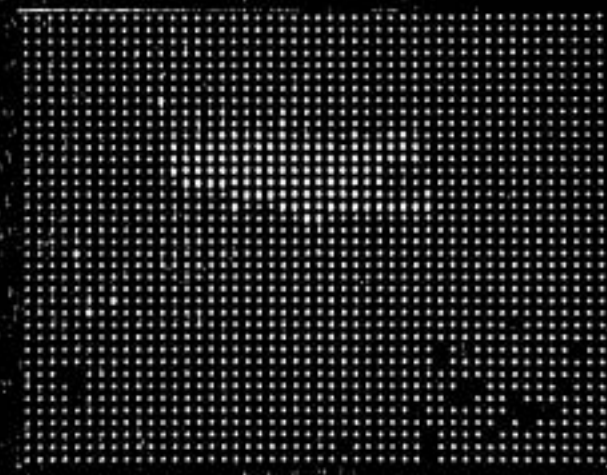
- 37.4 MS



- 34.8 MS



- 32.2 MS



- 29.5 MS





- 27.9 MS



- 24.3 MS



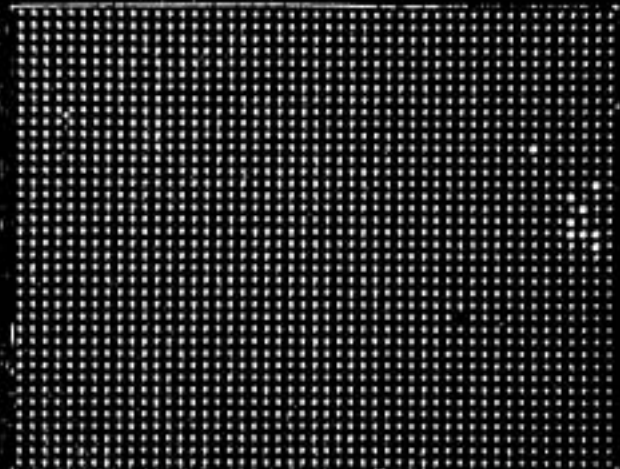
- 21.7 MS



- 19.1 MS



- 16.5 MS



- 14.0 MS